ISSN: 0975-833X

Available online at http://www.journalcra.com

International Journal of Current Research
Vol. 8, Issue, 02, pp.26617-26634 February, 2016

INTERNATIONAL JOURNAL OF CURRENT RESEARCH

RESEARCH ARTICLE

ANALYSIS OF MAGNETIC FIELD ON THE PERISTALTIC TRANSPORT OF JOHNSON-SEGALMAN FLUID IN AN INCLINED CHANNEL BOUNDED BY FLEXIBLE WALLS

[1]Naga Jyothi, N., [2,*]Devaki, P. and [3]Sreenadh, S.

[1]Department of Mathematics, Dravidian University, Kupam, A.P., India
[2]Department of Mathematics, MITS, Madanapalle, A.P., India
[3]Department of Mathematics, Sri Venkateswara University, Tirupati, A.P., India

ARTICLE INFO

Article History:
Received 25th November, 2015
Received in revised form
16th December, 2015
Accepted 21st January, 2016
Published online 27th February, 2016

Key words:
Magnetic field,
Peristaltic Transport,
Biofluid,
Johnson-Segalman Fluid,
Weisenberg Number.

ABSTRACT

In this paper we investigated the effect of magnetic field on the peristaltic transport of a biofluid in an inclined channel by modelling the fluid as a Johnson-Segalman fluid under the assumptions of low Reynolds number and long wavelength. The governing equations are solved using the perturbation technique. Stream function is determined and the relationship between velocity and the longitudinal pressure gradient is obtained. Further it is observed that the magnetic parameter M, Weissenberg number We, amplitude ratio ϕ and slip parameter a have strong effects on the velocity, stream function and the pressure gradient. The effects of these parameters on axial velocity, stream function and pressure gradient have been graphically studied. The pressure drops over a wave length are tabulated for some values of flux and magnetic parameter with small value of Weissenberg number. The results obtained for flow characteristics reveal many interesting behaviors that warrant further study on the non- Newtonian flow phenomena.

Citation: **Naga Jyothi, N., Devaki, P. and Sreenadh, S. 2016.** "Analysis of magnetic field on the peristaltic transport of johnson-segalman fluid in an inclined channel bounded by flexible walls", *International Journal of Current Research*, 8, (02), 26617-26634.

INTRODUCTION

The study of peristaltic flow has attracted many researchers in recent years. This is because of the fact that it is an inherent property of many syncytial smooth muscle tubes, stimulation at any point can cause a contractile ring to appear in the circular muscle of the gut, and this ring spreads along the tube. Peristaltic pumping is a form of fluid transport is a physiological mechanism in the human body that propels the fluids from one place to another. Peristaltic action is an inherent neuromuscular property of any tubular smooth muscle structure. The fluid is driven by a periodic progressive wave of contraction and expansion along the length of the distensible tube of uniform or varying cross-section. It is responsible for the transport of biological fluids in several physiological processes such as passage of urine from the kidneys to the bladder, the movement of chyme in the gastro-intestinal tract, transport of food bolus through the esophagus, transport of blood in small blood vessels, embryo transport in non-pregnant uterus, and movement of spermatozoa in human reproductive tract. Flawed/improper peristaltic motion in the ejaculatory duct may lead to retrograde ejaculation (ejaculation in which seminal fluid is discharged in the wrong direction, travelling up towards the bladder instead of outside the body through the urethra) a cause for infertility in men. Retrograde ejaculation is caused by diabetes, bladder neck surgery, alpha-antagonists, transurethral prostatectomy (TURP), colon or rectal surgery, multiple sclerosis, or spinal cord injury. These flows provide efficient means of sanitary fluid transport and are thus exploited in industrial peristaltic pumping and medical devices. For example, mechanical roller pumps are used to pump viscous fluids in the printing industry and the peristaltic transport of noxious fluid is performed in the nuclear industry. In addition, modern medical devices have been designed on the principle of peristaltic pumping to transport fluids without internal moving parts, for example, the blood in the heart-lung machine.

****Corresponding author: Devaki, P.,***
Department of Mathematics, MITS, Madanapalle, A.P., India.

Kwang Hua Chu (2003) discussed initiability problems related to the basic slip flow induced by peristaltic waves propagating along the deformable walls of the micro channels based on the spectral method. Mekheimer and Abd-Elmaboud (2008) discussed the influence of an endoscope on the peristaltic flow of a couple stress fluids in an annulus under a zero Reynolds number and long wavelength approximations. The effect of heat transfer on the peristaltic flow of a Newtonian fluid through a porous space in a vertical asymmetric channel is analyzed by Mekheimer *et al*. (2010). The peristaltic flow of Herschel-Bulkley fluid in an inclined flexible channel lined with porous material is investigated by Sreenadh *et al*. (2011). Krishna Kumari *et al*. (2011) studied the peristaltic pumping of a Jeffrey fluid under the effect of magnetic field in an inclined channel. The effect of slip on peristaltic transport of an incompressible Newtonian fluid in a two-dimensional inclined channel with wall effects has been investigated by Ramana Kumari and Radhakrishnamacharya (2011). Hina *et al*. (2012) investigated the peristaltic motion of a Maxwell fluid in an asymmetric complaint channel. The peristaltic flow of a Prandtl fluid in an asymmetric channel has been investigated by Akbar *et al*. (2012).

The subject of biomagnetic fluid dynamics has become more and more evident during the past few decades. The magnetohydrodynamic (MHD) flow of a fluid in a channel with elastic, rhythmically contracting walls (peristaltic flow) is of interest in connection with certain problems of the movement of conductive physiological fluids, (for example, the blood pump machines). The examples include the development of magnetic devices for cell separations, targeted transport of drugs using magnetic particles as drug carriers, magnetic wound or cancer tumour treatment causing magnetic hyperthermia, reduction of bleeding during surgeries etc. The magnerohydrodynamic (MHD) flows of non-Newtonian fluids are of great interest in magnetotherepy. The non-invasive radiological test uses a magnetic field (not radiation) to evaluate organs in abdomen prior to surgery in the small intestine (but not always).

Ebaid (2008) studied a new numerical solution for the MHD peristaltic flow of a biofluid with variable viscosity in a circular cylindrical tube by an Adomian decomposition method. Nadeem and Akbar (2010) have investigated the peristaltic flow of an incompressible MHD Newtonian fluid in a vertical annulus. The MHD peristaltic flow of an incompressible viscous fluid in an inclined asymmetric channel is investigated by Rami Reddy *et al*. (2010). Hayat and Noreen (2010) investigated the influence of an induced magnetic field on the peristaltic flow of an incompressible fourth grade fluid in a symmetric channel with heat transfer. Hemadri Reddy *et al*. (2011) studied the effect of induced magnetic field on peristaltic pumping of a Carreau fluid in an inclined symmetric channel filled with porous material under the long wavelength and low Reynolds number assumptions. The MHD peristaltic flow of a Prandtl fluid in a uniform channel under the assumptions of long wavelength and low Reynolds number is investigated by Jothi *et al*. (2012). Akram *et al*. (2013) studied Numerical and analytical treatment on peristaltic flow of Williamson fluid in the occurrence of induced magnetic field.

Although there are many models to describe non-Newtonian behavior of the fluids but in recent years, the Johnson-Segalman fluid has acquired a special status, as it includes the classical Newtonian fluid and Maxwell fluid as special cases. The Johnson-Segalman model was developed to allow for non-affine deformations. This model has been used by a number of researchers to explain the phenomenon “spurt”. “Spurt” is a phenomenon found in the flow of a number of non-Newtonian fluids in which there is a large increase in the volume throughout for a small increase in the driving pressure gradient, at a critical pressure gradient. Some experiments relevant to this issue have also been carried out by El Shahed *et al*. (2005) have investigated the peristaltic transport of Johnson-Segalman fluid by means of an infinite train of sinusoidal waves travelling along the walls of a two-dimensional flexible channel.

The fluid is electrically conducted by a magnetic field. A perturbation solution is obtained for the case in which amplitude ratio is small. A mathematical model for MHD flow of a Johnson-Segalman fluid in a channel with complaint walls is analyzed by Hayat *et al*. (2008a). Peristaltic transport of a Johnson-Segalman fluid in an asymmetric channel is studied by Hayat *et al*. (2008b). The flow is engendered due to sinusoidal waves on the channel walls. A series solution is developed for the case in which the amplitude ratio is small. Their assumptions show that the mean axial velocity of a Johnson-Segalman fluid is smaller than that of a viscous fluid.

The effect of magnetic field on the peristaltic motion of a Johnson-Segalman fluid in an asymmetric channel is investigated by Suryanarayana Reddy and Sankar Shekar Raju (2010). Nadeem and Akbar (2010) have analyzed the interaction of peristalsis with heat transfer for a Johnson-Segalman fluid in an inclined asymmetric channel under the supposition of long wavelength. Nadeem and Akbar (2011) studied the problem of heat and mass transfer on peristaltic flow of a Johnson-Segalman fluid in a vertical asymmetric channel under the effect of induced magnetic field. Recently, Hina *et al*. (2012) investigated the peristaltic flow of an incompressible Johnson-Segalman fluid in a curved channel. Effects of the channel wall properties are taken into account in this study. Peristaltic Motion of Johnson-Segalman Fluid in a Curved Channel with Slip Conditions was studied by Sadia Hina *et al*. (2014). In view of the above facts, much work was not done on inclined channels.

It is required more attention for investigations on inclined channels. In this paper we investigated the effect of magnetic field on the peristaltic transport of a biofluid in an inclined channel by modeling the fluid as a Johnson-Segalman fluid under the assumptions of low Reynolds number and long wavelength. Analytical solutions for the stream function and average velocity and pressure gradient have been obtained and the effects of various relevant parameters have been graphically studied.

The pressure differences over a wave length are tabulated for various values of flux and magnetic parameter with small value of Weissenberg number.

Basic Equations

The basic equations governing the flow of an incompressible fluid are the field equations

$$\text{div}V = 0, \quad \text{div}\sigma + \rho f = \rho \frac{dV}{dt} \tag{1}$$

where V is the velocity, f the body force per unit mass, ρ the density, $\frac{d}{dt}$ the material time derivative, and σ is the Cauchy stress. Johnson and Segalman proposed an integral model which can also be written in the rate-type form. With an appropriate choice of kernel function and the time constants, the Cauchy stress σ in such a Johnson-Segalman fluid is related to the fluid motion through

$$\sigma = pI + T \tag{2}$$

$$T = 2\mu D + S \tag{3}$$

$$S + m\left[\frac{dS}{dx} + S(W \quad aD) + (W \quad aD)^T S\right] = 2\eta D \tag{4}$$

where D is the symmetric part of the velocity gradient and W the skew-symmetric part of the velocity gradient, that is,

$$D = \frac{1}{2}[L + L^T], \quad W = \frac{1}{2}[L \quad L^T], \quad L = gradV \tag{5}$$

Also, pI denotes the indeterminate part of the stress due to the constraint of incompressibility, μ and η are viscosities, m is the relaxation time, and a is the slip parameter. When $a = 1$, the Johnson-Segalman model reduces to the Oldroyd-B model; when $a = 1$and $\mu = 0$, the Johnson-Segalman model reduces to the Maxwell fluid; and when m = 0, the model reduces to the classical Navier-Stokes fluid. Note that the bracketed term on the left-hand side of (2.4) is an objective time derivative.

Formulation and Solution of the problem

Consider a two-dimensional inclined channel of uniform width $2n$ filled with an incompressible Johnson-Segalman fluid. We choose a rectangular coordinate system for the channel with $\bar{X}$ along the center line and $\bar{Y}$ normal to it. The channel is inclined at an angle β with the horizontal.Let $\bar{U}$ and $\bar{V}$ be the longitudinal and transversal velocity components of the fluid, respectively. We assume that an infinite train of sinusoidal waves progresses with velocity along the walls in the $\bar{X}$ direction. (Fig.1)
The geometry of the wall surface is defined as

$$\bar{}(\bar{X}, t) = n + b\, sin\left(\frac{2\pi}{\lambda}(\bar{X}, t)\right) \tag{6}$$

where b is the amplitude and λ is the wavelength. We also assume that there is no motion of the wall in the longitudinal direction (extensible or elastic wall). For unsteady two-dimensional flows,

$$V = \bar{U}[(\bar{X}, \bar{Y}, t), \bar{V}(\bar{X}, \bar{Y}, t), 0] \tag{7}$$

The equations of motion (1) and the constitutive relations (2), (3) and (4) in the absence of body forces takes the following form:

$$\frac{\partial \bar{U}}{\partial \bar{X}} + \frac{\partial \bar{V}}{\partial \bar{Y}} = 0 \tag{8}$$

$$\rho\left(\frac{\partial}{\partial \mathrm{t}} + \bar{\mathrm{U}}\,\frac{\partial}{\partial \bar{\mathrm{X}}} + \bar{\mathrm{V}}\frac{\partial}{\partial \bar{\mathrm{Y}}}\right)\bar{\mathrm{U}} = \quad \frac{\partial \bar{\mathrm{P}}\,(\bar{\mathrm{X}}, \bar{\mathrm{Y}}, \mathrm{t})}{\partial \bar{\mathrm{X}}} + \mu\left(\frac{\partial^2}{\partial \bar{\mathrm{X}}^2} + \frac{\partial^2}{\partial \bar{\mathrm{Y}}^2}\right)\bar{\mathrm{U}} + \frac{\partial \bar{\mathrm{S}}_{\bar{\mathrm{X}}\bar{\mathrm{X}}}}{\partial \bar{\mathrm{X}}} + \frac{\partial \bar{\mathrm{S}}_{\bar{\mathrm{X}}\,\bar{\mathrm{Y}}}}{\partial \bar{\mathrm{X}}} \quad \sigma \mathrm{B_o}^2 \bar{\mathrm{U}} + \rho g \sin\beta \tag{9}$$

$$\rho\left(\frac{\partial}{\partial t} + \bar{U}\,\frac{\partial}{\partial \bar{X}} + \bar{V}\frac{\partial}{\partial \bar{Y}}\right)\bar{V} = \quad \frac{\partial \bar{P}\,(\bar{X}, \bar{Y}, t)}{\partial \bar{X}} + \mu\left(\frac{\partial^2}{\partial \bar{X}^2} + \frac{\partial^2}{\partial \bar{Y}^2}\right)\bar{V} + \frac{\partial \bar{S}_{\bar{X}\bar{Y}}}{\partial \bar{X}} + \frac{\partial \bar{S}_{\bar{Y}\bar{Y}}}{\partial \bar{X}} \quad \rho g \cos\beta \tag{10}$$

$$2\eta\frac{\partial\bar{U}}{\partial\bar{X}}+\bar{S}_{\bar{X}\bar{X}}+m\left(\frac{\partial}{\partial t}+\bar{U}\ \frac{\partial}{\partial\bar{X}}+\bar{V}\frac{\partial}{\partial\bar{Y}}\right)\bar{S}_{\bar{X}\bar{X}}\quad 2am\bar{S}_{\bar{X}\bar{X}}\frac{\partial\bar{U}}{\partial\bar{X}}+m\left[(1\quad a)\frac{\partial\bar{V}}{\partial\bar{X}}\quad(1+a)\frac{\partial\bar{U}}{\partial\bar{Y}}\right]\bar{S}_{\bar{X}\bar{Y}}$$
(11)

$$\eta\left(\frac{\partial\bar{U}}{\partial\bar{Y}}+\frac{\partial\bar{V}}{\partial\bar{X}}\right)=\bar{S}_{\bar{X}\bar{Y}}+m\left(\frac{\partial}{\partial t}+\bar{U}\ \frac{\partial}{\partial\bar{X}}+\bar{V}\frac{\partial}{\partial\bar{Y}}\right)\bar{S}_{\bar{X}\bar{Y}}+\frac{m}{2}\left[(1\quad a)\frac{\partial\bar{U}}{\partial\bar{Y}}\quad(1+a)\frac{\partial\bar{V}}{\partial\bar{X}}\right]\bar{S}_{\bar{X}\bar{X}}+\frac{m}{2}\left[(1\quad a)\frac{\partial\bar{V}}{\partial\bar{X}}\quad(1+a)\frac{\partial\bar{U}}{\partial\bar{Y}}\right]\bar{S}_{\bar{Y}\bar{Y}}\qquad(12)$$

$$2\,\eta\frac{\partial\bar{V}}{\partial\bar{Y}}=\bar{S}_{\bar{Y}\bar{Y}}+m\left(\frac{\partial}{\partial t}+\bar{U}\ \frac{\partial}{\partial\bar{X}}+\bar{V}\frac{\partial}{\partial\bar{Y}}\right)\bar{S}_{\bar{Y}\bar{Y}}\quad 2am\,\bar{S}_{\bar{Y}\bar{Y}}\frac{\partial\bar{V}}{\partial\bar{Y}}+m\left[(1\quad a)\frac{\partial\bar{U}}{\partial\bar{Y}}+(1+a)\frac{\partial\bar{V}}{\partial\bar{X}}\right]\bar{S}_{\bar{X}\bar{Y}}\qquad(13)$$

In the fixed coordinate system $(\bar{X},\bar{Y})$ the motion is unsteady because of the moving boundary. In a coordinate system $(\bar{x},\bar{y})$ moving with speed c, it can be treated as steady because the boundary shape appears to be stationary. The transformation between the frames is given by

$$\bar{x}=\bar{X}\quad ct\ ;\qquad \bar{y}=\bar{Y};\qquad \bar{u}=\bar{U}\quad c;\qquad \bar{v}=\bar{V}\qquad(14)$$

where $(\bar{u}\ ,\bar{v})$ are the components of the velocity in the moving coordinate system.

We use the following non-dimensional variables

$$x=\frac{2\pi}{\lambda}\bar{x};\quad y=\frac{\bar{y}}{n};\quad u=\frac{\bar{u}}{c}\ ;\quad v=\frac{\bar{v}}{c}\ ;\quad S=\frac{\eta}{\mu c}\bar{S}\ ;\quad p=\frac{2\pi n^2}{\lambda(\mu+\eta)c}\bar{p}\ ;\quad =\frac{\bar{h}}{n}\qquad(15)$$

where the wavelength λ is the characteristic longitudinal length. Substituting (14) into (8) to (13) and then using dimensionless variables (15), we arrive at

$$\delta\frac{\partial u}{\partial x}+\frac{\partial v}{\partial y}=0\qquad(16)$$

$$Re\left[\left(\delta u\frac{\partial}{\partial x}+v\frac{\partial}{\partial y}\right)u\right]=\quad\left(\frac{\eta+\mu}{\mu}\right)\frac{\partial p}{\partial x}+\left(\delta^2\frac{\partial^2}{\partial x^2}+\frac{\partial^2}{\partial y^2}\right)u+\delta\frac{\partial S_{xx}}{\partial x}+\frac{\partial S_{xy}}{\partial y}\quad M^2(u+1)+\xi\sin\beta$$
(17)

$$\delta Re\left[\left(\delta u\frac{\partial}{\partial x}+v\frac{\partial}{\partial y}\right)v\right]=\quad\left(\frac{\eta+\mu}{\mu}\right)\frac{\partial p}{\partial y}+\delta\left(\delta^2\frac{\partial^2}{\partial x^2}+\frac{\partial^2}{\partial y^2}\right)v+\delta^2\frac{\partial S_{xy}}{\partial x}+\ \delta\frac{\partial S_{yy}}{\partial y}\quad\delta\xi\cos\beta$$
(18)

$$\delta\left(\frac{2\eta}{\mu}\right)\frac{\partial u}{\partial x}=S_{xx}+We\left[\delta u\frac{\partial}{\partial x}+v\frac{\partial}{\partial y}\right]S_{xx}\quad 2aWe\delta\frac{\partial u}{\partial x}S_{xx}\ +We$$
$$\left[\delta(1\quad a)\frac{\partial v}{\partial x}\quad(1+a)\frac{\partial u}{\partial y}\right]S_{xy}\qquad(19)$$

$$\frac{\eta}{\mu}\left(\frac{\partial u}{\partial y}+\delta\frac{\partial v}{\partial x}\right)=S_{xy}+We\left[\delta u\frac{\partial}{\partial x}+v\frac{\partial}{\partial y}\right]S_{xy}+\frac{We}{2}\left[(1\quad a)\frac{\partial u}{\partial y}+\delta(1+a)\frac{\partial v}{\partial x}\right]S_{xx}+\frac{We}{2}\left[\delta(1\quad a)\frac{\partial v}{\partial x}\quad(1+a)\frac{\partial u}{\partial y}\right]S_{yy}$$
(20)

$$\left(\frac{2\eta}{\mu}\right)\frac{\partial v}{\partial y}=S_{yy}+We\left[\delta u\frac{\partial}{\partial x}+v\frac{\partial}{\partial y}\right]S_{yy}\quad 2WeaS_{yy}\frac{\partial v}{\partial y}+\ We\ \left[(1\quad a)\frac{\partial u}{\partial y}\quad\delta(1+a)\frac{\partial v}{\partial x}\right]S_{xy}\qquad(21)$$

in which the dimensionless wave number δ, the Reynolds number Re, and the Weisenberg number We are defined, respectively, as

$$\delta=\frac{2\pi n}{\lambda},\quad Re=\frac{\rho cn}{\mu},\quad We=\frac{mc}{n}$$

Equation (16) allows the introduction of the dimensionless stream function $\Psi(x,y)$ in terms of

$$u=\frac{\partial\Psi}{\partial y},\qquad v=\quad\delta\frac{\partial\Psi}{\partial x}$$

In terms of Ψ, we find that (16) is identically satisfied, while the other equations take the form

$$\delta Re\left[\left(\frac{\partial\Psi}{\partial y}\frac{\partial}{\partial x}\quad\frac{\partial\Psi}{\partial x}\frac{\partial}{\partial y}\right)\frac{\partial\Psi}{\partial y}\right]=\quad\left(\frac{\eta+\mu}{\mu}\right)\frac{\partial p}{\partial x}+\left(\delta^2\frac{\partial^3\Psi}{\partial x^2\partial y}+\frac{\partial^3\Psi}{\partial y^3}\right)u+\delta\frac{\partial S_{xx}}{\partial x}+\frac{\partial S_{xy}}{\partial y}\quad M^2\left(\frac{\partial\Psi}{\partial y}+1\right)+\xi\ \sin\beta$$
(22)

$$\delta^3 Re\left[\left(\frac{\partial\Psi}{\partial y}\frac{\partial}{\partial x} \quad \frac{\partial\Psi}{\partial x}\frac{\partial}{\partial y}\right)\frac{\partial\Psi}{\partial x}\right] = \quad \left(\frac{\eta+\mu}{\mu}\right)\frac{\partial p}{\partial y} \quad \delta^2\left(\delta^2\frac{\partial^3\Psi}{\partial x^3}+\frac{\partial^3\Psi}{\partial x\partial y^2}\right)v+\delta^2\frac{\partial S_{xy}}{\partial x}+\delta\frac{\partial S_{yy}}{\partial y} \quad \delta\xi\ \cos\beta \tag{23}$$

$$\left(\frac{2\eta\delta}{\mu}\right)\frac{\partial^2\Psi}{\partial x\partial y} = S_{xx}+We\delta\left[\frac{\partial\Psi}{\partial y}\frac{\partial}{\partial x} \quad \frac{\partial\Psi}{\partial x}\frac{\partial}{\partial y}\right]S_{xx} \quad 2aWe\delta\frac{\partial^2\Psi}{\partial x\partial y}S_{xx} \quad We\left[\delta^2(1 \quad a)\frac{\partial^2\Psi}{\partial x^2}+(1+a)\frac{\partial^2\Psi}{\partial y^2}\right]S_{xy} \tag{24}$$

$$\frac{\eta}{\mu}\left(\frac{\partial^2\Psi}{\partial y^2} \quad \delta^2\frac{\partial^2\Psi}{\partial x^2}\right) = S_{xy}+We\,\delta\left[\frac{\partial\Psi}{\partial y}\frac{\partial}{\partial x} \quad \frac{\partial\Psi}{\partial x}\frac{\partial}{\partial y}\right]S_{xy}+\frac{We}{2}\left[(1 \quad a)\frac{\partial^2\Psi}{\partial y^2}+\delta^2(1+a)\frac{\partial^2\Psi}{\partial x^2}\right]S_{xx} \quad \frac{We}{2}\left[\delta^2(1 \quad a)\frac{\partial^2\Psi}{\partial x^2}+(1+a)\frac{\partial^2\Psi}{\partial y^2}\right]S_{yy} \tag{25}$$

$$\left(\frac{2\eta\delta}{\mu}\right)\frac{\partial^2\Psi}{\partial x\partial y} = S_{yy}+We\delta\left[\frac{\partial\Psi}{\partial y}\frac{\partial}{\partial x} \quad \frac{\partial\Psi}{\partial x}\frac{\partial}{\partial y}\right]S_{yy}+2WeaS_{yy}\frac{\partial^2\Psi}{\partial x\partial y}+We\left[(1 \quad a)\frac{\partial^2\Psi}{\partial y^2}+\delta^2(1+a)\frac{\partial^2\Psi}{\partial x^2}\right]S_{xy} \tag{26}$$

Rate of Volume Flow and Boundary Conditions

The dimensional rate of fluid flow in the fixed frame is given by

$$Q = \int_0^{\bar{h}}\bar{U}(\bar{X},\bar{Y},t)\,d\bar{Y} \tag{27}$$

where $^{-}$ is a function of $\bar{X}$ and t. The rate of fluid flow in the moving frame is given by

$$q = \int_0^{\bar{h}}\bar{u}\,(\bar{x},\bar{y})d\bar{y}, \tag{28}$$

where $^{-}$ is a function of $\bar{x}$ alone. With the help of (14) and (15), one can show that these two rates related through

$$Q = q + c^{-} \tag{29}$$

The time-averaged flow over a period T at a fixed position $\bar{X}$ is given by

$$\bar{Q} = \frac{1}{T}\int_0^T Q\ dt. \tag{30}$$

Substituting (29) into (30), we find that

$$\bar{Q} = Q + cn \tag{31}$$

If we define the dimensionless time averaged flows Θ and F, respectively, in the fixed and moving frame as

$$\Theta = \frac{\bar{Q}}{cn}, \qquad F = \frac{q}{cn} \tag{32}$$

we find that (2.31) reduces to

$$\Theta = F + 1 \tag{33}$$

where

$$F = \int_0^h\frac{\partial\Psi}{\partial y}\,dy = \Psi(\ ) \quad \Psi(0) \tag{34}$$

If we choose the zero value of the streamline along the centre line ($y = 0$)

$$\Psi(0) = 0 \tag{35}$$

Then the shape of the wave is given by the streamline of value

$$\Psi(\ ) = F \tag{36}$$

The boundary conditions for the dimensionless stream function in the moving frame are

$\Psi = 0$, $\frac{\partial^2 \Psi}{\partial y^2} = 0$ on the centre line $y = 0$ (37)

$\frac{\partial \Psi}{\partial y} =$ 1 , $\Psi = F$ at the wall $y =$ (38)

We also note that h represents the dimensionless form of the surface of the peristaltic wall given by

$(x) = 1 + \Phi \sin x$ (39)

where

$\Phi = \frac{b}{n}$ (40)

is the amplitude ratio or the occlusion and $0 < \Phi < 1$.

Equations for Large Wave Length

A general solution of the dynamic equations (22)-(26) for arbitrary values of all parameters seems to be impossible to find. Accordingly, we carry out our investigation on the basis that the dimensionless wave number δ is small, that is,

$\delta \ll 1,$ (41)

which corresponds to the long-wavelength approximations Thus, to lowest order in δ, equations (22)-(26) gives

$\left(\frac{\eta+\mu}{\mu}\right)\frac{\partial p}{\partial x} = \frac{\partial S_{xy}}{\partial y} + \frac{\partial^3 \Psi}{\partial y^3}$ $M^2\left(\frac{\partial \Psi}{\partial y} + 1\right) + \xi \sin\beta$ (42)

$\frac{\partial p}{\partial y} = 0$ (43)

S_{xx} $We(1+a)\frac{\partial^2 \Psi}{\partial y^2} S_{xy} = 0$ (44)

$\left(\frac{\eta}{\mu}\right)\frac{\partial^2 \Psi}{\partial y^2} = S_{xy} + \frac{We}{2}(1$ $a)\frac{\partial^2 \Psi}{\partial y^2} S_{xx}$ $\frac{We}{2}(1+a)\frac{\partial^2 \Psi}{\partial y^2} S_{yy}$ (45)

$S_{yy} + We(1$ $a)\frac{\partial^2 \Psi}{\partial y^2} S_{xy} = 0$ (46)

Substituting (44) and (46) into (45) yields

$$S_{xy} = \frac{\left(\frac{\eta}{\mu}\right)\frac{\partial^2 \Psi}{\partial y^2}}{1 + We^2(1-a^2)\frac{\partial^2 \Psi^2}{\partial y^2}}$$ (47)

We note that from equation (43) that $p \neq p(y)$. The elimination of the pressure from (42) and (43) yields

$$\frac{\partial^2}{\partial y^2}\left[\frac{\left(\frac{\eta}{\mu}+1\right)\frac{\partial^2 \Psi}{\partial y^2} + We^2(1-a^2)\left(\frac{\partial^2 \Psi}{\partial y^2}\right)^3}{1 + We^2(1-a^2)\left(\frac{\partial^2 \Psi}{\partial y^2}\right)^2} \quad M^2\Psi\right] = 0$$ (48)

With the help of (47), the equation (42) takes the form

$$\left(\frac{\eta+\mu}{\mu}\right)\frac{\partial p}{\partial x} = \frac{\partial}{\partial y}\left[\frac{\left(\frac{\eta}{\mu}\right)\frac{\partial^2 \Psi}{\partial y^2}}{1 + We^2(1-a^2)\frac{\partial^2 \Psi^2}{\partial y^2}}\right] + \frac{\partial^3 \Psi}{\partial y^3} \quad M^2\left(\frac{\partial \Psi}{\partial y} + 1\right) + \xi \sin\beta$$ (49)

Perturbation Solution

For small values of We^2, (48) and (49) can be written using binomial theorem as

$$\frac{\partial^2}{\partial y^2}\left[\frac{\partial^2\Psi}{\partial y^2} + We^2\alpha_1\left(\frac{\partial^2\Psi}{\partial y^2}\right)^3 + We^4\alpha_2\left(\frac{\partial^2\Psi}{\partial y^2}\right)^5 \quad M^2\alpha_3\Psi\right] = 0 \tag{50}$$

$$\frac{\partial p}{\partial x} = \frac{\partial^3\Psi}{\partial y^3} + We^2\alpha_1\frac{\partial}{\partial y}\left(\frac{\partial^2\Psi}{\partial y^2}\right)^3 + We^4\alpha_2\frac{\partial}{\partial y}\left(\frac{\partial^2\Psi}{\partial y^2}\right)^5 \quad M^2\alpha_3\left(\frac{\partial\Psi}{\partial y} + 1\right) + \alpha_3\xi\sin\beta \tag{51}$$

where the dimensionless parameters α_1, α_2 and α_3 are defined as

$$\alpha_1 = \left(\frac{(a^2-1)\eta}{\eta+\mu}\right), \quad \alpha_2 = \left(\frac{(a^2-1)^2\eta}{\eta+\mu}\right), \quad \alpha_3 = \left(\frac{\mu}{\eta+\mu}\right) \tag{52}$$

Now we find the solution for (50) and (51) with boundary conditions (37) and (38) for a small Weisenberg number. We may expand flow quantities in a power series of We^2. We write the stream functionΨ, the pressure field P, and the flow rate F in the following form

$$\begin{aligned}\Psi &= \Psi_0 + We^2\Psi_1 + We^4\Psi_2 + \quad ,\\ P &= P_0 + We^2P_1 + We^4P_2 + \quad ,\\ F &= F_0 + We^2F_1 + We^4F_2 + \quad ,\end{aligned} \tag{53}$$

If we substitute (53) into (37), (38), (43), (50), and (51), and separate the terms of different orders in We^2 we obtain the following systems of partial differential equations for the stream function and pressure gradient together with the boundary conditions.

System of order We^0

The following system of equations of zeroth order is as follows:

$$\frac{\partial^4\Psi_0}{\partial y^4} \quad M^2\alpha_3\frac{\partial^2\Psi_0}{\partial y^2} = 0 \tag{54a}$$

$$\frac{\partial p_0}{\partial x} = \frac{\partial^3\Psi_0}{\partial y^3} \quad M^2\alpha_3\left(\frac{\partial\Psi_0}{\partial y} + 1\right) + \alpha_3\xi\sin\beta \tag{54b}$$

$$\frac{\partial p_0}{\partial y} = 0 \tag{54c}$$

with the boundary conditions

$$\Psi_0 = 0, \quad \frac{\partial^2\Psi_0}{\partial y^2} = 0 \quad \text{at} \quad y = 0 \tag{55a}$$

$$\Psi_0 = F_0, \quad \frac{\partial\Psi_0}{\partial y} = \quad 1 \quad \text{at} \quad y = \tag{55b}$$

System of order We^2

The first order differential equations are

$$\frac{\partial^4\Psi_1}{\partial y^4} \quad M^2\alpha_3\left(\frac{\partial^2\Psi_1}{\partial y^2}\right) = \quad \alpha_1\frac{\partial^2}{\partial y^2}\left[\left(\frac{\partial^2\Psi_0}{\partial y^2}\right)^3\right] \tag{56a}$$

$$\frac{\partial p_1}{\partial x} = \frac{\partial^3\Psi_1}{\partial y^3} + \alpha_1\frac{\partial}{\partial y}\left[\left(\frac{\partial^2\Psi_0}{\partial y^2}\right)^3\right] \quad M^2\alpha_3\frac{\partial\Psi_1}{\partial y} \tag{56b}$$

$$\frac{\partial p_1}{\partial y} = 0 \tag{56c}$$

with the boundary conditions

$$\Psi_1 = 0, \quad \frac{\partial^2\Psi_1}{\partial y^2} = 0 \quad \text{at} \quad y = 0 \tag{57a}$$

$$\Psi_1 = F_1, \quad \frac{\partial\Psi_1}{\partial y} = 0 \quad \text{at} \quad y = \tag{57b}$$

System of order We^4

The system of equations of second order is composed of

$$\frac{\partial^4 \Psi_2}{\partial y^4} \quad M^2 \alpha_3 \frac{\partial^2 \Psi_2}{\partial y^2} = \quad 3\alpha_1 \frac{\partial^2}{\partial y^2}\left[\left(\frac{\partial^2 \Psi_0}{\partial y^2}\right)^2 \frac{\partial^2 \Psi_1}{\partial y^2}\right] \quad \alpha_2 \frac{\partial^2}{\partial y^2}\left[\left(\frac{\partial^2 \Psi_0}{\partial y^2}\right)^5\right] \tag{58a}$$

$$\frac{\partial p_2}{\partial x} = \frac{\partial^3 \Psi_2}{\partial y^3} \quad M^2 \alpha_3 \frac{\partial \Psi_2}{\partial y} + 3\alpha_1 \frac{\partial}{\partial y}\left[\left(\frac{\partial^2 \Psi_0}{\partial y^2}\right)^2 \frac{\partial^2 \Psi_1}{\partial y^2}\right] + \alpha_2 \frac{\partial}{\partial y}\left[\left(\frac{\partial^2 \Psi_0}{\partial y^2}\right)^5\right] \tag{58b}$$

$$\frac{\partial p_2}{\partial y} = 0 \tag{58c}$$

with the boundary conditions

$$\Psi_2 = 0, \quad \frac{\partial^2 \Psi_2}{\partial y^2} = 0 \quad \text{at} \quad y = 0 \tag{59a}$$

$$\Psi_2 = F_2, \quad \frac{\partial \Psi_2}{\partial y} = 0 \quad \text{at} \quad y = \tag{59b}$$

In this system, further corrections due to the Johnson-Segalman constitutive equation enter. We seek to solve the sequence of problems at each order and generate thereby the series solution.

Zeroth order solution

The solution to the zeroth-order problem (54) subject to the boundary conditions (55) is given by

$$\Psi_0 = \left(\frac{F_0 M\sqrt{\alpha_3} + \tanh M\sqrt{\alpha_3}\, h}{hM\sqrt{\alpha_3} - \tanh M\sqrt{\alpha_3}\, h}\right)\left(y \quad \frac{\sinh M\sqrt{\alpha_3}\, y}{M\sqrt{\alpha_3}\cosh M\sqrt{\alpha_3}\, h}\right) \quad \frac{\sinh M\sqrt{\alpha_3}\, y}{M\sqrt{\alpha_3}\cosh M\sqrt{\alpha_3}\, h} \tag{60}$$

$$u_0 = \left(\frac{F_0 M\sqrt{\alpha_3} + \tanh M\sqrt{\alpha_3}\, h}{hM\sqrt{\alpha_3} - \tanh M\sqrt{\alpha_3}\, h}\right)\left[1 \quad \frac{\cosh M\sqrt{\alpha_3}\, y}{\cosh M\sqrt{\alpha_3}\, h}\right] \quad \frac{\cosh M\sqrt{\alpha_3}\, y}{\cosh M\sqrt{\alpha_3}\, h} \tag{61}$$

From the second and third equations in (54), it is clear that the transverse pressure gradient is zero and the longitudinal pressure gradient is given by

$$\frac{dp_0}{dx} = \quad M^2 \alpha_3 \left[\frac{F_0 M\sqrt{\alpha_3} + \tanh M\sqrt{\alpha_3}\, h}{hM\sqrt{\alpha_3} - \tanh M\sqrt{\alpha_3}\, h} + 1\right] + \alpha_3 \xi \sin\beta \tag{62}$$

The pressure rise per wavelength (ΔP_{λ_0}) in the longitudinal direction can be evaluated on the axis at $y = 0$. Thus, at the zeroth order, we have

$$\Delta P_{\lambda_0} = \int_0^{2\pi} \frac{dp_0}{dx} dx$$

First order solution

Substituting the zeroth-order solution into (56) the system of We^2 reduces the first equation as

$$\frac{\partial^4 \Psi_1}{\partial y^4} \quad M^2 \alpha_3 \left(\frac{\partial^2 \Psi_1}{\partial y^2}\right) = \quad \frac{\partial^2}{\partial y^2}\left(\frac{dp_0}{dx} \quad \alpha_3 \xi \sin\beta\right)^3 \left(\frac{\alpha_1 \sinh^3 M\sqrt{\alpha_3}\, y}{M^3 \alpha_3^{\frac{3}{2}} \cosh^3 M\sqrt{\alpha_3}\, h}\right) \tag{63}$$

On solving the above equation with boundary conditions (57), the expression for the stream function Ψ_1 the axial velocity u_1 is given by

$$\Psi_1 = y\left(H_0 M\sqrt{\alpha_3}\cosh M\sqrt{\alpha_3}\,h + \left(\frac{dp_0}{dx} - \alpha_3\xi\sin\beta\right)^3\left(\frac{3\alpha_1\cosh 3M\sqrt{\alpha_3}\,h}{32M^4\alpha_3^{\,2}\cosh^3 M\sqrt{\alpha_3}\,h} - \frac{3\alpha_1}{8M^4\alpha_3^{\,2}\cosh^2 M\sqrt{\alpha_3}\,h} - \frac{3\alpha_1 h\sinh M\sqrt{\alpha_3}\,h}{8M^3\alpha_3^{\frac{3}{2}}\cosh^3 M\sqrt{\alpha_3}\,h}\right)\right) - H_0\sinh M\sqrt{\alpha_3}\,y - \left(\frac{dp_0}{dx} - \alpha_3\xi\sin\beta\right)^3\left(\frac{\alpha_1\sinh 3M\sqrt{\alpha_3}\,y}{32M^5\alpha_3^{\frac{5}{2}}\cosh^3 M\sqrt{\alpha_3}\,h} - \frac{3\alpha_1 y\cosh M\sqrt{\alpha_3}\,y}{8M^4\alpha_3^{\,2}\cosh^3 M\sqrt{\alpha_3}\,h}\right) \tag{64}$$

$$u_1 = H_0 M\sqrt{\alpha_3}\cosh M\sqrt{\alpha_3}\,h + \left(\frac{dp_0}{dx} - \alpha_3\xi\sin\beta\right)^3\left(\frac{3\alpha_1\cosh 3M\sqrt{\alpha_3}\,h}{32M^4\alpha_3^{\,2}\cosh^3 M\sqrt{\alpha_3}\,h} - \frac{3\alpha_1}{8M^4\alpha_3^{\,2}\cosh^2 M\sqrt{\alpha_3}\,h} - \frac{3\alpha_1 h\sinh M\sqrt{\alpha_3}\,h}{8M^3\alpha_3^{\frac{3}{2}}\cosh^3 M\sqrt{\alpha_3}\,h}\right) - H_0 M\sqrt{\alpha_3}\cosh M\sqrt{\alpha_3}\,y - \left(\frac{dp_0}{dx} - \alpha_3\xi\sin\beta\right)^3\left(\frac{3\alpha_1\cosh 3M\sqrt{\alpha_3}\,y}{32M^4\alpha_3^{\,2}\cosh^3 M\sqrt{\alpha_3}\,h} - \frac{3\alpha_1 y\sinh M\sqrt{\alpha_3}\,y}{8M^3\alpha_3^{\frac{3}{2}}\cosh^3 M\sqrt{\alpha_3}\,h} - \frac{3\alpha_1\cosh M\sqrt{\alpha_3}\,y}{8M^4\alpha_3^{\,2}\cosh^3 M\sqrt{\alpha_3}\,h}\right) \tag{65}$$

Using the zeroth-order solution in the second equation of (56), along with the boundary conditions (57), the longitudinal pressure gradient turn out to be

$$\frac{dp_1}{dx} = M^2\alpha_3\left(\frac{dp_0}{dx} - \alpha_3\xi\sin\beta\right)^3\left(\frac{3\alpha_1\cosh 3M\sqrt{\alpha_3}\,h}{32M^4\alpha_3^{\,2}\cosh^3 M\sqrt{\alpha_3}\,h} - \frac{3\alpha_1}{8M^4\alpha_3^{\,2}\cosh^2 M\sqrt{\alpha_3}\,h} - \frac{3\alpha_1 h\sinh M\sqrt{\alpha_3}\,h}{8M^3\alpha_3^{\frac{3}{2}}\cosh^3 M\sqrt{\alpha_3}\,h}\right) - M^3\alpha_3^{\frac{3}{2}}H_0 M\sqrt{\alpha_3}\cosh M\sqrt{\alpha_3}\,h \tag{66}$$

where

$$H_0 = \frac{1}{hM\sqrt{\alpha_3} - \tanh M\sqrt{\alpha_3}\,h}\left(F_1 - \left(\frac{dp_0}{dx} - \alpha_3\xi\sin\beta\right)^3\left(\frac{3\alpha_1 h\cosh 3M\sqrt{\alpha_3}\,h}{32M^4\alpha_3^{\,2}\cosh^3 M\sqrt{\alpha_3}\,h} - \frac{\alpha_1\sinh 3M\sqrt{\alpha_3}\,h}{32M^5\alpha_3^{\frac{5}{2}}\cosh^3 M\sqrt{\alpha_3}\,h} - \frac{3\alpha_1 h^2\sinh M\sqrt{\alpha_3}\,h}{8M^3\alpha_3^{\frac{3}{2}}\cosh^3 M\sqrt{\alpha_3}\,h}\right)\right) \tag{67}$$

The pressure rise per wavelength (ΔP_{λ_1}) in the longitudinal direction can be evaluated on the axis at $y = 0$. Thus, at the first order, we have

$$\Delta P_{\lambda_1} = \int_0^{2\pi}\frac{dp_1}{dx}\,dx$$

Second order solution

If we insert the zeroth-order and first-order solutions into (62), we get

$$\frac{\partial^4\Psi_2}{\partial y^4} - M^2\alpha_3\left(\frac{\partial^2\Psi_2}{\partial y^2}\right) = \frac{\partial^2}{\partial y^2}\left(\left(\frac{dp_0}{dx} - \alpha_3\xi\sin\beta\right)^2\left(\frac{3\alpha_1 H_0 \sinh 3M\sqrt{\alpha_3}\,y}{4\cosh^2 M\sqrt{\alpha_3}\,h} - \frac{9\alpha_1 H_0 \sinh M\sqrt{\alpha_3}\,y}{4\cosh^2 M\sqrt{\alpha_3}\,h}\right) + \left(\frac{dp_0}{dx} - \alpha_3\xi\sin\beta\right)^5\left(\frac{27\alpha_1^2\sinh 5M\sqrt{\alpha_3}\,y}{128M^5\alpha_3^{\frac{5}{2}}\cosh^5 M\sqrt{\alpha_3}\,h} - \frac{63\alpha_1^2\sinh 3M\sqrt{\alpha_3}\,y}{64M^5\alpha_3^{\frac{5}{2}}\cosh^5 M\sqrt{\alpha_3}\,h} - \frac{9\alpha_1^2 y\cosh 3M\sqrt{\alpha_3}\,y}{32M^4\alpha_3^2\cosh^5 M\sqrt{\alpha_3}\,h} + \frac{9\alpha_1^2 y\cosh M\sqrt{\alpha_3}\,y}{32M^4\alpha_3^2\cosh^5 M\sqrt{\alpha_3}\,h}\right) - \left(\frac{dp_0}{dx} - \alpha_3\xi\sin\beta\right)^5\left(\frac{\alpha_2\sinh 5M\sqrt{\alpha_3}\,y}{16M^5\alpha_3^{\frac{5}{2}}\cosh^5 M\sqrt{\alpha_3}\,h} - \frac{5\alpha_2\sinh 3M\sqrt{\alpha_3}\,y}{16M^5\alpha_3^{\frac{5}{2}}\cosh^5 M\sqrt{\alpha_3}\,h} + \frac{5\alpha_2\sinh M\sqrt{\alpha_3}\,y}{8M^5\alpha_3^{\frac{5}{2}}\cosh^5 M\sqrt{\alpha_3}\,h}\right)\right) \tag{68}$$

Solving (68), subject to the boundary conditions (65), we find, after lengthy calculations, the stream function and axial velocity at this order are:

$$\Psi_2 = y\left(-H_1 M\sqrt{\alpha_3}\cosh M\sqrt{\alpha_3}\,h - \left(\frac{dp_0}{dx} - \alpha_3\xi\sin\beta\right)^2\left(\frac{9\alpha_1 H_0\cosh 3M\sqrt{\alpha_3}\,h}{32\,M\sqrt{\alpha_3}\cosh^2 M\sqrt{\alpha_3}\,h} - \frac{9\alpha_1 H_0 h\sinh M\sqrt{\alpha_3}\,h}{8\cosh^2 M\sqrt{\alpha_3}\,h} - \frac{9\alpha_1 H_0}{8\,M\sqrt{\alpha_3}\cosh M\sqrt{\alpha_3}\,h}\right) - \left(\frac{dp_0}{dx} - \alpha_3\xi\sin\beta\right)^5\left(\frac{45\alpha_1^2\cosh 5M\sqrt{\alpha_3}\,y}{1024M^7\alpha_3^{\frac{7}{2}}\cosh^5 M\sqrt{\alpha_3}\,h} - \frac{333\alpha_1^2\cosh 3M\sqrt{\alpha_3}\,h}{1024M^6\alpha_3^3\cosh^5 M\sqrt{\alpha_3}\,h} + \frac{261\alpha_1^2 h\sinh M\sqrt{\alpha_3}\,h}{256M^5\alpha_3^{\frac{5}{2}}\cosh^5 M\sqrt{\alpha_3}\,h} + \frac{225\alpha_1^2}{256M^6\alpha_3^3\cosh^4 M\sqrt{\alpha_3}\,h} - \frac{9\alpha_1^2 h^2}{128M^4\alpha_3^2\cosh^4 M\sqrt{\alpha_3}\,h} - \frac{27\alpha_1^2 h\sinh 3M\sqrt{\alpha_3}\,h}{256M^5\alpha_3^{\frac{5}{2}}\cosh^5 M\sqrt{\alpha_3}\,h}\right) + \left(\frac{dp_0}{dx} - \alpha_3\xi\sin\beta\right)^5\left(\frac{5\alpha_2\cosh 5M\sqrt{\alpha_3}\,h}{384M^6\alpha_3^3\cosh^5 M\sqrt{\alpha_3}\,h} - \frac{15\alpha_2\cosh 3M\sqrt{\alpha_3}\,h}{128M^6\alpha_3^3\cosh^5 M\sqrt{\alpha_3}\,h} + \frac{5\alpha_2}{16M^6\alpha_3^3\cosh^4 M\sqrt{\alpha_3}\,h} + \frac{5\alpha_2 h\sinh M\sqrt{\alpha_3}\,h}{16M^5\alpha_3^{\frac{5}{2}}\cosh^5 M\sqrt{\alpha_3}\,h}\right)\right) + H_1\sinh M\sqrt{\alpha_3}\,y + \left(\frac{dp_0}{dx} - \alpha_3\xi\sin\beta\right)^2\left(\frac{3\alpha_1 H_0\sinh 3M\sqrt{\alpha_3}\,y}{32\,M^2\alpha_3\cosh^2 M\sqrt{\alpha_3}\,h} - \frac{9\alpha_1 H_0\, y\cosh M\sqrt{\alpha_3}\,y}{8M\sqrt{\alpha_3}\cosh^2 M\sqrt{\alpha_3}\,h}\right) + \left(\frac{dp_0}{dx} - \alpha_3\xi\sin\beta\right)^5\left(\frac{9\alpha_1^2\sinh 5M\sqrt{\alpha_3}\,y}{1024M^6\alpha_3^3\cosh^5 M\sqrt{\alpha_3}\,h} - \frac{99\alpha_1^2\sinh 3M\sqrt{\alpha_3}\,y}{1024M^7\alpha_3^{\frac{7}{2}}\cosh^5 M\sqrt{\alpha_3}\,h} + \frac{225\alpha_1^2 y\cosh M\sqrt{\alpha_3}\,y}{256M^6\alpha_3^3\cosh^5 M\sqrt{\alpha_3}\,h} + \frac{9\alpha_1^2 y^2\sinh M\sqrt{\alpha_3}\,y}{128M^5\alpha_3^{\frac{5}{2}}\cosh^5 M\sqrt{\alpha_3}\,h} - \frac{9\alpha_1^2 y\cosh 3M\sqrt{\alpha_3}\,y}{256M^6\alpha_3^3\cosh^5 M\sqrt{\alpha_3}\,h}\right) - \left(\frac{dp_0}{dx} - \alpha_3\xi\sin\beta\right)^5\left(\frac{\alpha_2\sinh 5M\sqrt{\alpha_3}\,y}{384M^7\alpha_3^{\frac{7}{2}}\cosh^5 M\sqrt{\alpha_3}\,h} - \frac{5\alpha_2\sinh 3M\sqrt{\alpha_3}\,y}{128M^7\alpha_3^{\frac{7}{2}}\cosh^5 M\sqrt{\alpha_3}\,h} + \frac{5\alpha_2 y\cosh M\sqrt{\alpha_3}\,y}{16M^6\alpha_3^3\cosh^5 M\sqrt{\alpha_3}\,h}\right) \tag{69}$$

$$u_2 = -H_1 M\sqrt{\alpha_3}\cosh M\sqrt{\alpha_3}\,h - \left(\frac{dp_0}{dx} - \alpha_3\xi\sin\beta\right)^2\left(\frac{9\alpha_1 H_0\cosh 3M\sqrt{\alpha_3}\,h}{32\,M\sqrt{\alpha_3}\cosh^2 M\sqrt{\alpha_3}\,h} - \frac{9\alpha_1 H_0 h\sinh M\sqrt{\alpha_3}\,h}{8\cosh^2 M\sqrt{\alpha_3}\,h} - \frac{9\alpha_1 H_0}{8\,M\sqrt{\alpha_3}\cosh M\sqrt{\alpha_3}\,h}\right) - \left(\frac{dp_0}{dx} - \alpha_3\xi\sin\beta\right)^5\left(\frac{45\alpha_1^2\cosh 5M\sqrt{\alpha_3}\,y}{1024M^7\alpha_3^{\frac{7}{2}}\cosh^5 M\sqrt{\alpha_3}\,h} - \frac{333\alpha_1^2\cosh 3M\sqrt{\alpha_3}\,h}{1024M^6\alpha_3^3\cosh^5 M\sqrt{\alpha_3}\,h} + \frac{261\alpha_1^2 h\sinh M\sqrt{\alpha_3}\,h}{256M^5\alpha_3^{\frac{5}{2}}\cosh^5 M\sqrt{\alpha_3}\,h} + \frac{225\alpha_1^2}{256M^6\alpha_3^3\cosh^4 M\sqrt{\alpha_3}\,h} - \frac{9\alpha_1^2 h^2}{128M^4\alpha_3^2\cosh^4 M\sqrt{\alpha_3}\,h} - \frac{27\alpha_1^2 h\sinh 3M\sqrt{\alpha_3}\,h}{256M^5\alpha_3^{\frac{5}{2}}\cosh^5 M\sqrt{\alpha_3}\,h}\right) + \left(\frac{dp_0}{dx} - \alpha_3\xi\sin\beta\right)^5\left(\frac{5\alpha_2\cosh 5M\sqrt{\alpha_3}\,h}{384M^6\alpha_3^3\cosh^5 M\sqrt{\alpha_3}\,h} - \frac{15\alpha_2\cosh 3M\sqrt{\alpha_3}\,h}{128M^6\alpha_3^3\cosh^5 M\sqrt{\alpha_3}\,h} + \frac{5\alpha_2}{16M^6\alpha_3^3\cosh^4 M\sqrt{\alpha_3}\,h} + \frac{5\alpha_2 h\sinh M\sqrt{\alpha_3}\,h}{16M^5\alpha_3^{\frac{5}{2}}\cosh^5 M\sqrt{\alpha_3}\,h}\right) + H_1\sinh M\sqrt{\alpha_3}\,y\left(\frac{dp_0}{dx} - \alpha_3\xi\sin\beta\right)^2\left(\frac{3\alpha_1 H_0\sinh 3M\sqrt{\alpha_3}\,y}{32\,M^2\alpha_3\cosh^2 M\sqrt{\alpha_3}\,h} - \frac{9\alpha_1 H_0 y\cosh M\sqrt{\alpha_3}\,y}{8M\sqrt{\alpha_3}\cosh^2 M\sqrt{\alpha_3}\,h}\right) + \left(\frac{dp_0}{dx} - \alpha_3\xi\sin\beta\right)^5\left(\frac{9\alpha_1^2\sinh 5M\sqrt{\alpha_3}\,y}{1024M^6\alpha_3^3\cosh^5 M\sqrt{\alpha_3}\,h} - \frac{99\alpha_1^2\sinh 3M\sqrt{\alpha_3}\,y}{1024M^7\alpha_3^{\frac{7}{2}}\cosh^5 M\sqrt{\alpha_3}\,h} + \frac{225\alpha_1^2 y\cosh M\sqrt{\alpha_3}\,y}{256M^6\alpha_3^3\cosh^5 M\sqrt{\alpha_3}\,h} + \frac{9\alpha_1^2 y^2\sinh M\sqrt{\alpha_3}\,y}{128M^5\alpha_3^{\frac{5}{2}}\cosh^5 M\sqrt{\alpha_3}\,h} - \frac{9\alpha_1^2 y\cosh 3M\sqrt{\alpha_3}\,y}{256M^6\alpha_3^3\cosh^5 M\sqrt{\alpha_3}\,h}\right) - \left(\frac{dp_0}{dx} - \alpha_3\xi\sin\beta\right)^5\left(\frac{\alpha_2\sinh 5M\sqrt{\alpha_3}\,y}{384M^7\alpha_3^{\frac{7}{2}}\cosh^5 M\sqrt{\alpha_3}\,h} - \frac{5\alpha_2\sinh 3M\sqrt{\alpha_3}\,y}{128M^7\alpha_3^{\frac{7}{2}}\cosh^5 M\sqrt{\alpha_3}\,h} + \frac{5\alpha_2 y\cosh M\sqrt{\alpha_3}\,y}{16M^6\alpha_3^3\cosh^5 M\sqrt{\alpha_3}\,h}\right) \tag{70}$$

The longitudinal pressure gradient is given as

$$\frac{dP_2}{dx} = H_1 M^3\alpha_3^{\frac{3}{2}}\cosh M\sqrt{\alpha_3}\,h + \left(\frac{dP_0}{dx} - \alpha_3\xi\sin\beta\right)^2\left(\frac{9\alpha_1 H_0 M\sqrt{\alpha_3}\cosh 3M\sqrt{\alpha_3}\,h}{32\cosh^2 M\sqrt{\alpha_3}\,h} - \frac{9\alpha_1 H_0 M\sqrt{\alpha_3}}{8\cosh M\sqrt{\alpha_3}\,h} - \frac{9\alpha_1 H_0 M^2\alpha_3\sin M\sqrt{\alpha_3}\,h}{8\cosh^2 M\sqrt{\alpha_3}\,h}\right) + \left(\frac{dP_0}{dx} - \alpha_3\xi\sin\beta\right)^5\left(\frac{45\alpha_1^2\cosh 5M\sqrt{\alpha_3}h}{1024M^4\alpha_3^2\cosh^5 M\sqrt{\alpha_3}\,h} - \frac{333\alpha_1^2\cosh 3M\sqrt{\alpha_3}\,h}{1024M^4\alpha_3^2\cosh^5 M\sqrt{\alpha_3}\,h} + \frac{225\alpha_1^2}{256M^4\alpha_3^2\cosh^4 M\sqrt{\alpha_3}\,h} + \frac{261\alpha_1^2 h\sinh M\sqrt{\alpha_3}\,h}{256M^5\alpha_3^{\frac{5}{2}}\cosh^5 M\sqrt{\alpha_3}\,h} - \frac{27\alpha_1^2 h\sinh 3M\sqrt{\alpha_3}\,h}{256M^5\alpha_3^{\frac{5}{2}}\cosh^5 M\sqrt{\alpha_3}\,h} + \frac{9\alpha_1^2 h^2}{128M^2\alpha_3\cosh^4 M\sqrt{\alpha_3}\,h}\right) - \left(\frac{dP_0}{dx} - \alpha_3\xi\sin\beta\right)^5\left(\frac{5\alpha_2\cosh 5M\sqrt{\alpha_3}h}{384M^5\alpha_3^{\frac{5}{2}}\cosh^5 M\sqrt{\alpha_3}\,h} - \frac{15\alpha_2\cosh 3M\sqrt{\alpha_3}h}{128M^4\alpha_3^2\cosh^5 M\sqrt{\alpha_3}\,h} + \frac{5\alpha_2 h\sinh M\sqrt{\alpha_3}\,h}{16M^5\alpha_3^{\frac{5}{2}}\cosh^5 M\sqrt{\alpha_3}\,h} + \frac{5\alpha_2}{16M^4\alpha_3^2\cosh^4 M\sqrt{\alpha_3}\,h}\right) \tag{71}$$

where

$$H_1 = \frac{1}{hM\sqrt{\alpha_3} - \tanh M\sqrt{\alpha_3}\,h}\left(\left(\frac{dP_0}{dx} - \alpha_3\xi\sin\beta\right)^2\left(\frac{3\alpha_1 H_0\sinh 3M\sqrt{\alpha_3}\,h}{32M^2\alpha_3\cosh^2 M\sqrt{\alpha_3}\,h} - \frac{9\alpha_1 H_0 h\cosh 3M\sqrt{\alpha_3}\,h}{32\,M\sqrt{\alpha_3}\cosh^2 M\sqrt{\alpha_3}\,h} - \frac{3\alpha_1 H_0 M\sqrt{\alpha_3}\cosh 3M\sqrt{\alpha_3}\,h}{8\cosh^2 M\sqrt{\alpha_3}\,h}\right) + \left(\frac{dP_0}{dx} - \alpha_3\xi\sin\beta\right)^5\left(\frac{9\alpha_1^2\sinh 5M\sqrt{\alpha_3}h}{1024M^7\alpha_3^{\frac{7}{2}}\cosh^5 M\sqrt{\alpha_3}\,h} - \frac{45\alpha_1^2 h\cosh 5M\sqrt{\alpha_3}h}{1024M^6\alpha_3^3\cosh^5 M\sqrt{\alpha_3}\,h} - \frac{99\alpha_1^2\sinh 3M\sqrt{\alpha_3}h}{1024M^7\alpha_3^{\frac{7}{2}}\cosh^5 M\sqrt{\alpha_3}\,h} + \frac{27\alpha_1^2 h^2\sinh 3M\sqrt{\alpha_3}h}{256M^5\alpha_3^{\frac{5}{2}}\cosh^5 M\sqrt{\alpha_3}\,h} + \frac{297\alpha_1^2 h\cosh 3M\sqrt{\alpha_3}h}{1024M^6\alpha_3^3\cosh^5 M\sqrt{\alpha_3}\,h} - \frac{243\alpha_1^2 h^2\sinh M\sqrt{\alpha_3}h}{256M^5\alpha_3^{\frac{5}{2}}\cosh^5 M\sqrt{\alpha_3}\,h} - \frac{9\alpha_1^2 h^3}{128M^4\alpha_3^2\cosh^4 M\sqrt{\alpha_3}\,h}\right) - \left(\frac{dP_0}{dx} - \alpha_3\xi\sin\beta\right)^5\left(\frac{\alpha_2\sinh 5M\sqrt{\alpha_3}\,h}{384M^7\alpha_3^{\frac{7}{2}}\cosh^5 M\sqrt{\alpha_3}\,h} - \frac{5\alpha_2\sinh 3M\sqrt{\alpha_3}\,h}{128M^7\alpha_3^{\frac{7}{2}}\cosh^5 M\sqrt{\alpha_3}\,h} - \frac{5\alpha_2 h\cosh 5M\sqrt{\alpha_3}\,h}{384M^5\alpha_3^{\frac{5}{2}}\cosh^5 M\sqrt{\alpha_3}\,h} + \frac{15\alpha_2 h\cosh 3M\sqrt{\alpha_3}\,h}{128M^6\alpha_3^3\cosh^5 M\sqrt{\alpha_3}\,h} - \frac{5\alpha_2 h^2\sinh M\sqrt{\alpha_3}h}{256M^5\alpha_3^{\frac{5}{2}}\cosh^5 M\sqrt{\alpha_3}\,h}\right) - F_2\right) \tag{72}$$

The pressure rise per wavelength (ΔP_{λ_2}) in the longitudinal direction can be evaluated on the axis at $y = 0$. Thus, at second order, we have

$$\Delta P_{\lambda_2} = \int_0^{2\pi} \frac{dp_2}{dx}\, dx$$

Now we summarize the results of the perturbation series through the order We^4. The expressions for Ψ, u and $\frac{dp}{dx}$ may respectively take the following form

$$\Psi = \frac{F_0 M\sqrt{\alpha_3}\tanh M\sqrt{\alpha_3}h}{hM\sqrt{\alpha_3}-\tanh M\sqrt{\alpha_3}h}\left(y - \frac{\sinh M\sqrt{\alpha_3}y}{M\sqrt{\alpha_3}\cosh M\sqrt{\alpha_3}h}\right) - \frac{\sinh M\sqrt{\alpha_3}y}{M\sqrt{\alpha_3}\cosh M\sqrt{\alpha_3}h} +$$

$$We^2\left(y\left(H_0 M\sqrt{\alpha_3}\cosh M\sqrt{\alpha_3}h + \left(\frac{dp_0}{dx} - \alpha_3\xi\sin\beta\right)^3\left(\frac{3\alpha_1\cosh 3M\sqrt{\alpha_3}h}{32M^4\alpha_3^{\,2}\cosh^3 M\sqrt{\alpha_3}h} - \right.\right.\right.$$

$$\left.\left.\left.\frac{3\alpha_1}{8M^4\alpha_3^{\,2}\cosh^2 M\sqrt{\alpha_3}h} - \frac{3\alpha_1 h\sinh M\sqrt{\alpha_3}h}{8M^3\alpha_3^{\frac{5}{2}}\cosh^2 M\sqrt{\alpha_3}h}\right)\right) - H_0\sinh M\sqrt{\alpha_3}\,y -$$

$$\left.\left(\frac{dp_0}{dx} - \alpha_3\xi\sin\beta\right)^3\left(\frac{\alpha_1\sinh 3M\sqrt{\alpha_3}y}{32M^5\alpha_3^{\frac{5}{2}}\cosh^3 M\sqrt{\alpha_3}h} - \frac{3\alpha_1\cos hM\sqrt{\alpha_3}y}{8M^4\alpha_3^{\,2}\cosh^3 M\sqrt{\alpha_3}h}\right)\right) +$$

$$We^4\left(y\left(-H_1 M\sqrt{\alpha_3}\cos h\, M\sqrt{\alpha_3}h - \left(\frac{dp_0}{dx} - \alpha_3\xi\sin\beta\right)^2\left(\frac{9\alpha_1\cosh 3M\sqrt{\alpha_3}h}{32M\sqrt{\alpha_3}\cosh^2 M\sqrt{\alpha_3}h} - \right.\right.\right.$$

$$\frac{9\alpha_1 H_0 h\sin M\sqrt{\alpha_3}h}{8\cosh^2 M\sqrt{\alpha_3}h} - \left.\frac{9\alpha_1 H_0}{8M\sqrt{\alpha_3}\cos hM\sqrt{\alpha_3}h}\right) - \left(\frac{dp_0}{dx} - \alpha_3\xi\sin\beta\right)^5\left(\frac{45\alpha_1^{\,2}\cos h5M\sqrt{\alpha_3}y}{1024M^7\alpha_3^{\frac{7}{2}}\cosh^5 M\sqrt{\alpha_3}h} - \right.$$

$$\frac{333\alpha_1^{\,2}\cos h3M\sqrt{\alpha_3}h}{1024M^6\alpha_3^{\,3}\cosh^5 M\sqrt{\alpha_3}h} + \frac{261\alpha_1^{\,2}h\sin hM\sqrt{\alpha_3}h}{256M^5\alpha_3^{\frac{5}{2}}\cosh^5 M\sqrt{\alpha_3}h} + \frac{225\alpha_1^{\,2}}{256M^6\alpha_3^{\,3}\cosh^4 M\sqrt{\alpha_3}h} - \frac{9\alpha_1^{\,2}h^2}{128M^4\alpha_3^{\,2}\cosh^4 M\sqrt{\alpha_3}h} -$$

$$\left.\frac{27\alpha_1^{\,2}h\sin h3M\sqrt{\alpha_3}h}{256M^5\alpha_3^{\frac{5}{2}}\cosh^5 M\sqrt{\alpha_3}h}\right) + \left(\frac{dp_0}{dx} - \alpha_3\xi\sin\beta\right)^5\left(\frac{5\alpha_2\cosh 5M\sqrt{\alpha_3}h}{384M^6\alpha_3^{\,3}\cosh^5 M\sqrt{\alpha_3}h} - \frac{15\alpha_2\cosh 3M\sqrt{\alpha_3}h}{128M^6\alpha_3^{\,3}\cosh^5 M\sqrt{\alpha_3}h} + \right.$$

$$\left.\left.\frac{5\alpha_2}{16M^6\alpha_3^{\,3}\cosh^4 M\sqrt{\alpha_3}h} + \frac{5\alpha_2 h\sinh M\sqrt{\alpha_3}h}{16M^5\alpha_3^{\frac{5}{2}}\cosh^5 M\sqrt{\alpha_3}h}\right)\right) + H_1\sinh M\sqrt{\alpha_3}y +$$

$$\left(\frac{dp_0}{dx} - \alpha_3\xi\sin\beta\right)^2\left(\frac{3\alpha_1 H_0\sinh 3M\sqrt{\alpha_3}y}{32M^2\alpha_3\cosh^2 M\sqrt{\alpha_3}h} - \frac{9\alpha_1 H_0\, y\cosh M\sqrt{\alpha_3}y}{8M\sqrt{\alpha_3}\cosh^2 M\sqrt{\alpha_3}h}\right) + \left(\frac{dp_0}{dx} - \right.$$

$$\left.\alpha_3\xi\sin\beta\right)^5\left(\frac{9\alpha_1^{\,2}\sinh 5M\sqrt{\alpha_3}y}{1024M^6\alpha_3^{\,3}\cosh^5 M\sqrt{\alpha_3}h} - \frac{99\alpha_1^{\,2}\sinh 3M\sqrt{\alpha_3}y}{1024M^7\alpha_3^{\frac{7}{2}}\cosh^5 M\sqrt{\alpha_3}h} + \frac{225\alpha_1^{\,2}y\cosh M\sqrt{\alpha_3}y}{256M^6\alpha_3^{\,3}\cosh^5 M\sqrt{\alpha_3}h} + \right.$$

$$\frac{9\alpha_1^{\,2}y^2\sinh M\sqrt{\alpha_3}y}{128M^5\alpha_3^{\frac{5}{2}}\cosh^5 M\sqrt{\alpha_3}h} - \left.\frac{9\alpha_1^{\,2}y\cosh 3M\sqrt{\alpha_3}y}{256M^6\alpha_3^{\,3}\cosh^5 M\sqrt{\alpha_3}h}\right) - \left(\frac{dp_0}{dx} - \alpha_3\xi\sin\beta\right)^5\left(\frac{\alpha_2\sinh 5M\sqrt{\alpha_3}y}{384M^7\alpha_3^{\frac{7}{2}}\cosh^5 M\sqrt{\alpha_3}h} - \right.$$

$$\left.\left.\frac{5\alpha_2\sinh 3M\sqrt{\alpha_3}y}{128M^7\alpha_3^{\frac{7}{2}}\cosh^5 M\sqrt{\alpha_3}h} + \frac{5\alpha_2 y\cosh M\sqrt{\alpha_3}y}{16M^6\alpha_3^{\,3}\cosh^5 M\sqrt{\alpha_3}h}\right)\right) \tag{73}$$

$$u = \frac{F_0 M\sqrt{\alpha_3}\tanh M\sqrt{\alpha_3}h}{hM\sqrt{\alpha_3}-\tanh M\sqrt{\alpha_3}h}\left(1-\frac{\cosh M\sqrt{\alpha_3}y}{\cosh M\sqrt{\alpha_3}h}\right)-\frac{\cosh M\sqrt{\alpha_3}y}{\cosh M\sqrt{\alpha_3}h}+We^2\left(H_0M\sqrt{\alpha_3}\cosh M\sqrt{\alpha_3}h+\right.$$
$$\left(\frac{dp_0}{dx}-\alpha_3\xi\sin\beta\right)^3\left(\frac{3\alpha_1\cosh 3M\sqrt{\alpha_3}h}{32M^4{\alpha_3}^2\cosh^3 M\sqrt{\alpha_3}h}-\frac{3\alpha_1}{8M^4{\alpha_3}^2\cosh^2 M\sqrt{\alpha_3}h}-\frac{3\alpha_1 h\sinh M\sqrt{\alpha_3}h}{8M^3\alpha_3^{\frac{5}{2}}\cosh^3 M\sqrt{\alpha_3}h}\right)-$$
$$H_0M\sqrt{\alpha_3}\cosh M\sqrt{\alpha_3}y-\left(\frac{dp_0}{dx}-\alpha_3\xi\sin\beta\right)^3\left(\frac{3\alpha_1\cosh 3M\sqrt{\alpha_3}y}{32M^4{\alpha_3}^2\cosh^3 M\sqrt{\alpha_3}h}-\frac{3\alpha_1 y\sinh M\sqrt{\alpha_3}y}{8M^3\alpha_3^{\frac{5}{2}}\cosh^3 M\sqrt{\alpha_3}h}-\right.$$
$$\left.\left.\frac{3\alpha_1\cosh M\sqrt{\alpha_3}y}{8M^4{\alpha_3}^2\cosh^3 M\sqrt{\alpha_3}h}\right)\right)+$$
$$We^4\left(-H_1M\sqrt{\alpha_3}\cosh M\sqrt{\alpha_3}h-\right.$$
$$\left(\frac{dp_0}{dx}-\alpha_3\xi\sin\beta\right)^2\left(\frac{9\alpha_1H_0\cosh 3M\sqrt{\alpha_3}h}{32M\sqrt{\alpha_3}\cosh^2 M\sqrt{\alpha_3}h}-\frac{9\alpha_1H_0h\sinh M\sqrt{\alpha_3}h}{8\cosh^2 M\sqrt{\alpha_3}h}-\frac{9\alpha_1H_0}{8M\sqrt{\alpha_3}\cosh M\sqrt{\alpha_3}h}\right)-$$
$$\left(\frac{dp_0}{dx}-\alpha_3\xi\sin\beta\right)^5\left(\frac{45{\alpha_1}^2\cosh 5M\sqrt{\alpha_3}h}{1024M^6\alpha_3^3\cosh^5 M\sqrt{\alpha_3}h}-\frac{333{\alpha_1}^2\cosh 3M\sqrt{\alpha_3}h}{1024M^6\alpha_3^3\cosh^5 M\sqrt{\alpha_3}h}+\frac{225{\alpha_1}^2}{256M^6\alpha_3^3\cosh^4 M\sqrt{\alpha_3}h}+\right.$$
$$\frac{261{\alpha_1}^2\sinh M\sqrt{\alpha_3}h}{256M^5\alpha_3^{\frac{5}{2}}\cosh^5 M\sqrt{\alpha_3}h}-\frac{27{\alpha_1}^2\sinh 3M\sqrt{\alpha_3}h}{256M^5\alpha_3^{\frac{5}{2}}\cosh^5 M\sqrt{\alpha_3}h}+\left.\frac{9{\alpha_1}^2h^2}{128M^4{\alpha_3}^2\cosh^4 M\sqrt{\alpha_3}h}\right)+$$
$$\left(\frac{dp_0}{dx}-\alpha_3\xi\sin\beta\right)^5\left(\frac{5\alpha_2\cosh 5M\sqrt{\alpha_3}h}{384M^5\alpha_3^{\frac{5}{2}}\cosh^5 M\sqrt{\alpha_3}h}-\frac{15\alpha_2\cosh 3M\sqrt{\alpha_3}h}{128M^6\alpha_3^3\cosh^5 M\sqrt{\alpha_3}h}+\frac{5\alpha_2h\sinh M\sqrt{\alpha_3}h}{16M^5\alpha_3^{\frac{5}{2}}\cosh^5 M\sqrt{\alpha_3}h}+\right.$$
$$\left.\frac{5\alpha_2}{16M^6\alpha_3^3\cosh^5 M\sqrt{\alpha_3}h}\right)+H_1M\sqrt{\alpha_3}\cosh M\sqrt{\alpha_3}y+\left(\frac{dp_0}{dx}-\alpha_3\xi\sin\beta\right)^5\left(\frac{9\alpha_1H_0\cosh 3M\sqrt{\alpha_3}y}{32M\sqrt{\alpha_3}\cosh^2 M\sqrt{\alpha_3}h}-\right.$$
$$\frac{9\alpha_1H_0y\sinh M\sqrt{\alpha_3}y}{8\cosh^2 M\sqrt{\alpha_3}h}-\left.\frac{9\alpha_1H_0\cosh M\sqrt{\alpha_3}y}{8M\sqrt{\alpha_3}\cosh^2 M\sqrt{\alpha_3}h}\right)+\left(\frac{dp_0}{dx}-\alpha_3\xi\sin\beta\right)^5\left(\frac{45{\alpha_1}^2\cosh 5M\sqrt{\alpha_3}y}{1024M^6\alpha_3^3\cosh^5 M\sqrt{\alpha_3}h}-\right.$$
$$\frac{333{\alpha_1}^2\cosh 3M\sqrt{\alpha_3}y}{1024M^6\alpha_3^3\cosh^5 M\sqrt{\alpha_3}h}+\frac{261{\alpha_1}^2y\sinh M\sqrt{\alpha_3}y}{256M^5\alpha_3^{\frac{5}{2}}\cosh^5 M\sqrt{\alpha_3}h}+\frac{225{\alpha_1}^2\cosh M\sqrt{\alpha_3}y}{256M^5\alpha_3^{\frac{5}{2}}\cosh^5 M\sqrt{\alpha_3}h}-\frac{27{\alpha_1}^2\sinh 3M\sqrt{\alpha_3}y}{256M^5\alpha_3^{\frac{5}{2}}\cosh^5 M\sqrt{\alpha_3}h}+$$
$$\frac{9{\alpha_1}^2y^2\cosh M\sqrt{\alpha_3}y}{128M^4{\alpha_3}^2\cosh^5 M\sqrt{\alpha_3}h}\left.\right)-\left(\frac{dp_0}{dx}-\alpha_3\xi\sin\beta\right)^5\left(\frac{5\alpha_2\cosh 5M\sqrt{\alpha_3}y}{384M^5\alpha_3^{\frac{5}{2}}\cosh^5 M\sqrt{\alpha_3}h}-\frac{15\alpha_2\cosh 3M\sqrt{\alpha_3}y}{128M^6\alpha_3^3\cosh^5 M\sqrt{\alpha_3}h}+\right.$$
$$\left.\left.\frac{5\alpha_2y\sinh M\sqrt{\alpha_3}y}{16M^5\alpha_3^{\frac{5}{2}}\cosh^5 M\sqrt{\alpha_3}h}+\frac{5\alpha_2\cosh M\sqrt{\alpha_3}y}{16M^6\alpha_3^3\cosh^5 M\sqrt{\alpha_3}h}\right)\right) \tag{74}$$

$$\frac{dp}{dx}=-M^2\alpha_3\left(\frac{F_0M\sqrt{\alpha_3}+\tanh M\sqrt{\alpha_3}h}{hM\sqrt{\alpha_3}-\tanh M\sqrt{\alpha_3}h}+1\right)+\alpha_3\xi\sin\beta+We^2\left(-M^3\alpha_3^{\frac{5}{2}}H_0\cosh M\sqrt{\alpha_3}h-\right.$$
$$\left.\left(\frac{dp_0}{dx}-\alpha_3\xi\sin\beta\right)^3\left(\frac{3\alpha_1\cosh 3M\sqrt{\alpha_3}h}{32M^2\alpha_3\cosh^3 M\sqrt{\alpha_3}h}-\frac{3\alpha_1}{8M^2\alpha_3\cosh^2 M\sqrt{\alpha_3}h}-\frac{3\alpha_1h\sinh M\sqrt{\alpha_3}h}{8M\sqrt{\alpha_3}\cosh^3 M\sqrt{\alpha_3}h}\right)\right)+$$
$$We^4\left(H_1M^3\alpha_3^{\frac{5}{2}}\cosh M\sqrt{\alpha_3}h+M^2\alpha_3\left(\frac{dp_0}{dx}-\alpha_3\xi\sin\beta\right)^2\left(\frac{9\alpha_1H_0\cosh 3M\sqrt{\alpha_3}h}{32M\sqrt{\alpha_3}\cosh^2 M\sqrt{\alpha_3}h}-\right.\right.$$
$$\frac{9\alpha_1H_0}{8M\sqrt{\alpha_3}\cosh M\sqrt{\alpha_3}h}-\left.\frac{9\alpha_1H_0h\sinh M\sqrt{\alpha_3}h}{8\cosh^2 M\sqrt{\alpha_3}h}\right)+\left(\frac{dp_0}{dx}-\alpha_3\xi\sin\beta\right)^5\left(\frac{45{\alpha_1}^2\cosh 5M\sqrt{\alpha_3}h}{1024M^4{\alpha_3}^2\cosh^5 M\sqrt{\alpha_3}h}-\right.$$
$$\frac{333{\alpha_1}^2\cosh 3M\sqrt{\alpha_3}h}{1024M^4{\alpha_3}^2\cosh^5 M\sqrt{\alpha_3}h}+\frac{225{\alpha_1}^2}{256M^4{\alpha_3}^2\cosh^4 M\sqrt{\alpha_3}h}+\frac{261{\alpha_1}^2h\sinh M\sqrt{3}h}{256M^5\alpha_3^{\frac{5}{2}}\cosh^5 M\sqrt{\alpha_3}h}-\frac{27{\alpha_1}^2h\sinh 3M\sqrt{3}h}{256M^5\alpha_3^{\frac{5}{2}}\cosh^5 M\sqrt{\alpha_3}h}+$$
$$\frac{9{\alpha_1}^2h^2}{128M^2\alpha_3\cosh^4 M\sqrt{\alpha_3}h}\left.\right)-\left(\frac{dp_0}{dx}-\alpha_3\xi\sin\beta\right)^5\left(\frac{5\alpha_2\cosh 5M\sqrt{\alpha_3}h}{384M^5\alpha_3^{\frac{5}{2}}\cosh^5 M\sqrt{\alpha_3}h}-\frac{15\alpha_2\cosh 3M\sqrt{\alpha_3}h}{128M^4{\alpha_3}^2\cosh^5 M\sqrt{\alpha_3}h}+\right.$$
$$\left.\left.\frac{5\alpha_2\sinh M\sqrt{\alpha_3}h}{16M^5\alpha_3^{\frac{5}{2}}\cosh^5 M\sqrt{\alpha_3}h}+\frac{5\alpha_2}{16M^4{\alpha_3}^2\cosh^4 M\sqrt{\alpha_3}h}\right)\right) \tag{75}$$

RESULTS AND DISCUSSION

The main goal of this section lies in the analysis of significant parameters on u, ψ and $\frac{dp}{dx}$. Further the pressure rise per wave length at the channel walls are carefully analyzed through numerical integration.

To study the behavior of axial velocity u, numerical calculations for several values of magnetic parameter M, Weissenberg number We, amplitude ratio ϕ and slip parameter a are carried out. The effect of the magnetic parameter M on the velocity distribution can be seen through Fig (2). It is observed that the axial velocity decreases with increase in M. Fig (3) depicts that velocity decreases with increase in Weissenberg number We. From Fig (4) it is observed that velocity decreases as the amplitude ratio increases. Fig (5) shows that velocity increases as the value of slip parameter increases.

The variation of stream function Ψ for different values magnetic parameter M, Weissenberg number We, amplitude ratio ϕ and slip parameter a are carried out. From Fig (6) it is observed that the flow decreases as the value of M increases. Fig (7) depicts that the flow increases with the increase in the Weissenberg number We. The variation of the flow with the variation of amplitude ratio ϕ is seen in Fig (8). It shows that flow increases with increase in ϕ. From the Fig (9) it is observed that as slip parameter increases, flow decreases.

The variation of axial pressure gradient $\frac{dp}{dx}$ for different values of magnetic parameter M, Weissenberg number We, angle of inclination β, amplitude ratio ϕ and slip parameter a are carried out. Fig (10) depicts that the axial pressure gradient $\frac{dp}{dx}$ is increasing in the intervals (0.5, 1.0) & (1.5, 2.0), the pressure gradient is decreasing in the intervals (0, 0.5), (1.0, 1.5) & (2.0, 2.5) respectively with increase in the value of magnetic parameter M. The effect of Weissenberg number We on $\frac{dp}{dx}$ is seen through Fig (11).

It is observed that, as the Weissenberg number We increases, the axial pressure gradient is increasing in the in the intervals (0.5, 1.0) & (1.5, 2.0) but We has not much effect on $\frac{dp}{dx}$ in the intervals (0, 0.5), (1.0, 1.5) & (2.0, 2.5) respectively. The variation of axial pressure gradient $\frac{dp}{dx}$ with angle of inclination β is shown in Fig (12). It is observed that, the axial pressure gradient increases with increase in the value of β. From Fig (13) we can see that the axial pressure gradient is increasing in the intervals (0.5, 1.0) & (1.5, 2.0) as the value of amplitude ratio ϕ increases and ϕ has not much effect on pressure gradient in the intervals (0, 0.5), (1.0, 1.5) & (2.0, 2.5) respectively. Fig (14) shows the variation of the axial pressure gradient $\frac{dp}{dx}$ with slip parameter a. Here we observe that as a decreases, the pressure gradient $\frac{dp}{dx}$ is decreasing in the intervals (0.7, 0.8) & (1.7, 1.8) but with increase in slip parameter a there has not much effect on the pressure gradient $\frac{dp}{dx}$ in the intervals (0, 0.6), (0.8, 1.7) & (1.8, 2.5) respectively.

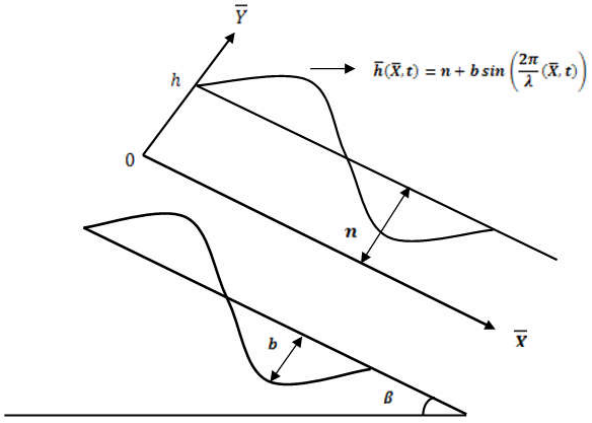

Fig 1. Schematic diagram of the inclined channel

Table 1: Pressure drop per wave length for various values of flux F and the magnetic parameter M. The other parameters are $\mu = 1, \eta = 1, a = 0.5, We = 0.05, \beta = \frac{\pi}{6}$ and $\phi = 0.4$

-0.5			-1.0			-2.0			-3.0		
0.10	0.12	0.14	0.10	0.12	0.14	0.10	0.12	0.14	0.10	0.12	0.14
5.65	1.20	- 0.15	6.58	2.15	0.79	8.49	4.05	2.69	10.38	5.95	4.29

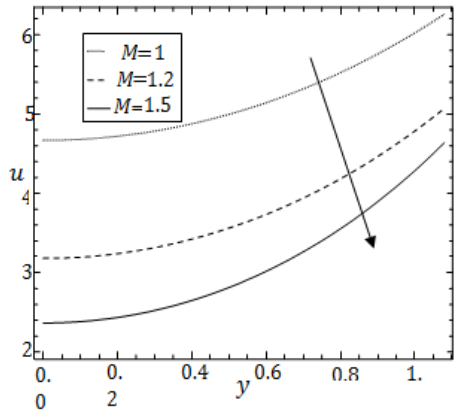

Fig. 2. Velocity profiles for different M with $a = 0.5; \eta = 1;\ \mu = 1;\ \ \xi = 1; \phi = 0.4;$ $We = 0.05; \beta = \frac{\pi}{6}; F_0 = -1; F_1 = 0; F_2 = -1;$

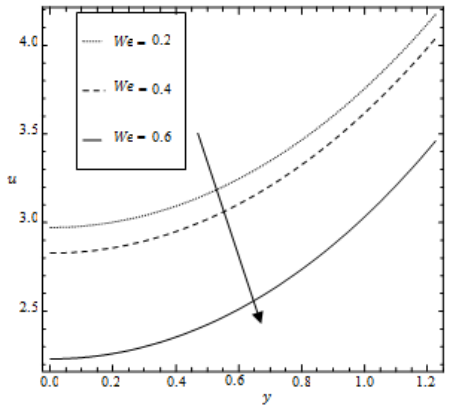

Fig. 3. Velocity profiles for different We with $a = 0.5; \eta = 1; \mu = 1; \xi = 1; M = 1; \phi = 0.4;$ $\beta = \frac{\pi}{6}; F_0 = -1; F_1 = 0; F_2 = -1;$

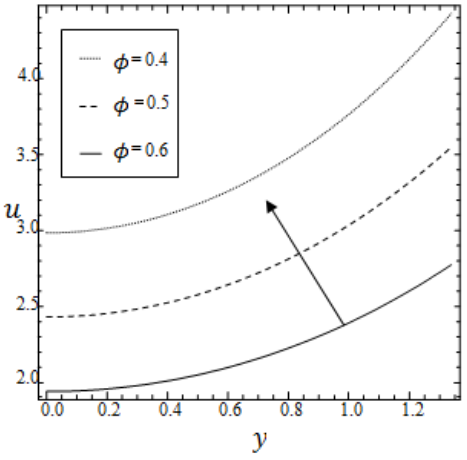

Fig. 4. Velocity profiles for different ϕ with $a = 0.5; \eta = 1; \mu = 1; \xi = 1;\ M = 1;$ $We = 0.05; \beta = \frac{\pi}{6}; F_0 = -1; F_1 = 0; F_2 = -1;$

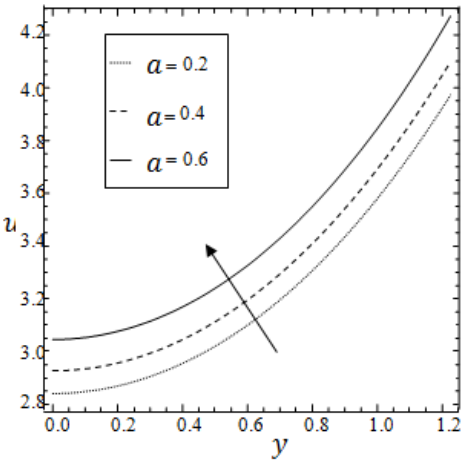

Fig. 5. Velocity profiles for different a with $\phi = 0.4, \eta = 1; \mu = 1; \xi = 1; M = 1;$ $We = 0.05; \beta = \frac{\pi}{6}; F_0 = -1; F_1 = 0; F_2 = -1;$

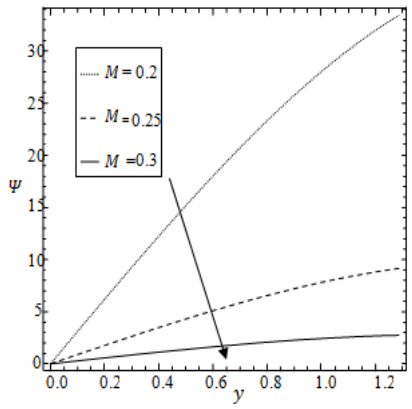

Fig. 6. Profiles of stream function for different M with $a = 0.2; \eta = 1; \mu = 1; \xi = 1; \phi = 0.4; We = 0.5;$ $\beta = \frac{\pi}{6}; F_0 = -1; F_1 = 0; F_2 = -1;$

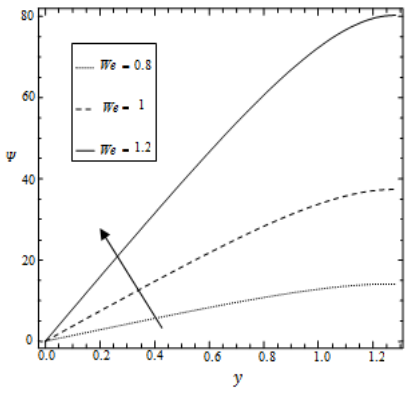

Fig. 7. Profiles of stream function for different We with $a = 0.2; \eta = 1; \mu = 1; \xi = 1; M = 5; \phi = 0.5;$ $\beta = \frac{\pi}{6}; F_0 = -1; F_1 = 0;\ F_2 = -1;$

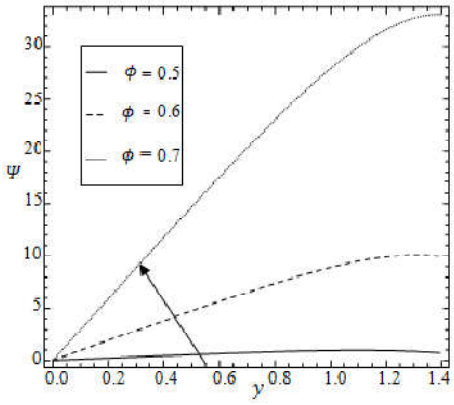

Fig. 8. Profiles of stream function for different ϕ with $a = 0.2; \eta = 1; \mu = 1; \xi = 1; We = 0.5; M = 5; \beta = \frac{\pi}{6}; F_0 = -1; F_1 =$

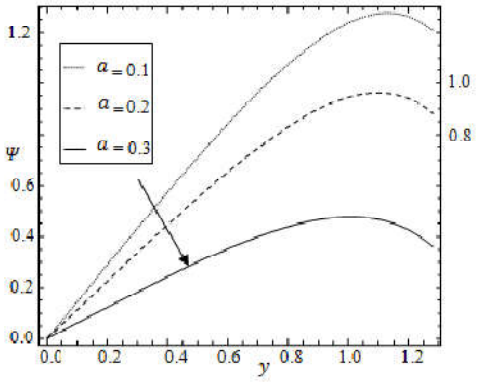

Fig. 9. Profiles of stream function for different a with $\eta = 1; \mu = 1; \xi = 1; M = 5; \phi = 0.5; \beta = \frac{\pi}{6}; We = 0.5; F_0 = -1; F_1 =$

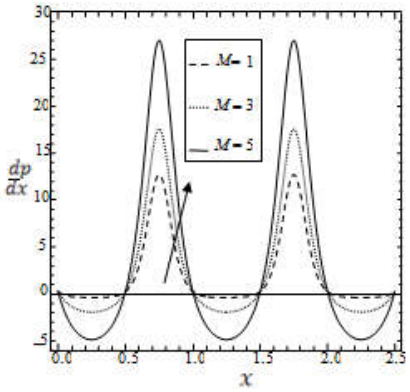

Fig. 10. Profiles of axial pressure gradient $\frac{dp}{dx}$ for different values of M with $a = 0.8; \eta = 1; \mu = 1; \xi = 1; \beta = \frac{\pi}{6}; We = 0.01; \phi = 0.5; F_0 = -1; F_1 = 0; F_2 = -1$

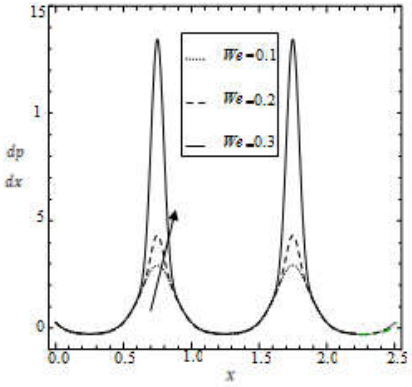

Fig. 11. Profiles of axial pressure gradient $\frac{dp}{dx}$ for different values of We with $a = 0.5; \eta = 1; \mu = 1; \xi = 1; \beta = \frac{\pi}{6}; \phi = 0.3; M = 1; F_0 = -1; F_1 = 0; F_2 = -1;$

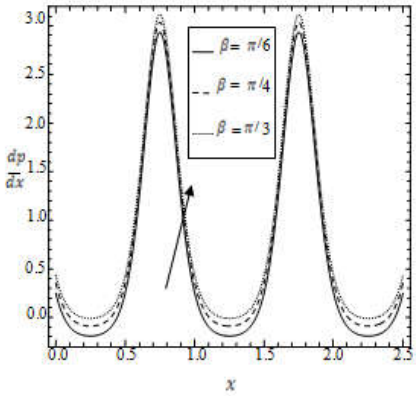

Fig. 12. Profiles of axial pressure gradient $\frac{dp}{dx}$ for different values of β with $a = 0.8; \eta = 1; \mu = 1; \xi = 1; M = 0.5; \phi = 0.3; We = 0.01; F_0 = -1; F_1 = 0; F_2 = -1;$

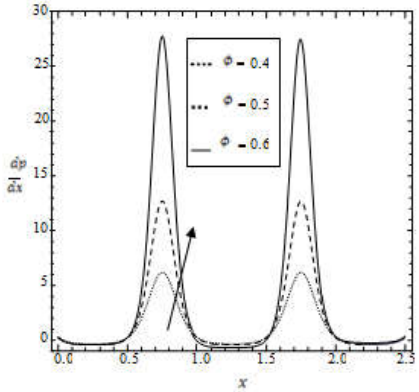

Fig. 13. Profiles of axial pressure gradient $\frac{dp}{dx}$ for different values of ϕ with $a = 0.8; \eta = 1; \mu = 1; \xi = 1; \beta = \frac{\pi}{6}; We = 0.01; M = 1; F_0 = -1; F_1 = 0; F_2 = -1;$

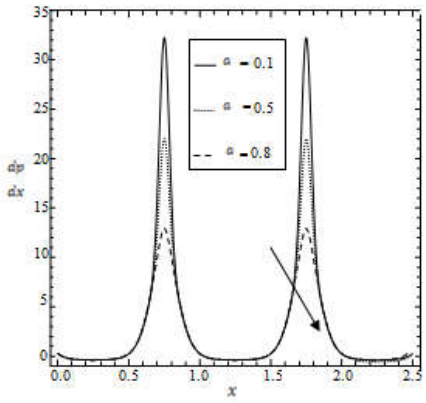

Fig 14: Profiles of axial pressure gradient $\frac{dp}{dx}$ for different values of a with $\eta = 1$; $\mu = 1; \xi = 1; M = 1; \phi = 0.5; We = 0.05; \beta = \frac{\pi}{6}; F_0 = -1;$ $F_1 = 0; F_2 = -1;$

The corresponding pressure drops in the flow direction over a wave length are listed in the Table 1 for some values of F and M with small value of Weissenberg number $We = 0.05$. It is observed that, the pressure drops decrease over a wavelength with increase in the values of the flux and the magnetic parameter.

REFERENCES

Akber, N. S., Nadeem, S. and Lee, C. 2012. Peristaltic flow of a Prandtl fluid model in an asymmetric channel, *International Journal of Physical Sciences*, 7 (5), 687-695.

Akram, S., Nadeem, S., Hanif, M. 2013. Numerical and analytical treatment on peristaltic flow of Williamson fluid in the occurrence of induced magnetic field, *J. Magnetism. Magnetic materials*, 346, 142-151.

El Shahed, M. and Haroun, M. H. 2005. Peristaltic transport of a Johnson-Segalman fluid under effect of a magnetic field, *Math. Prolb. Eng.,* 6, 663-677.

Hayat, T. Mariyam Javed, S. Asghar, M.H.D 2008a. Peristaltic motion of a Johnson-Segalman fluid in a channel with complaint walls, *Phys. Lett*. A 372 (30), 5026-5036.

Hayat, T. and Noreen, S. 2010. Peristaltic transport of fourth grade fluid with heat transfer and induced magnetic field. C. *R Mécanique,* 338, 518-528.

Hayat, T., Afsar, A. and Ali, N. 2008b. Peristaltic transport of a Johnson-Segalman fluid in an asymmetric channel, Math. *Comp. Model.,* 47, 380-400.

Hemadri Reddy, R., Kavitha, A., Sreenadh, S. and Saravana, R. 2011. Effect of induced magnetic field on peristaltic transport of a Carreau fluid in an inclined channel filled with porous material, *International Journal of Mechanical and Materials Engineering* , 6 (2), 240-249.

Hina, S., Hayat, T. and Asghar, S. 2012. Peristaltic transport of Johnson-Segalman fluid in a curved channel with Complaint walls, Non-liner Analysis: *Modelling and Controll*, 17 (3), 297-311.

Hina, S., Hayat, T., Asghar, S. and Obaidat, S. 2012. Peristaltic flow of a Maxwell fluid in an asymmetric channel with wall properties, *International Journal of Physical Sciences*, 7 (14), 2145-2155.

Hina, S., Mustafa, M. and Hayat, T. 2014. Peristaltic Motion of Johnson-Segalman Fluid in a Curved Channel with Slip Conditions, PLoS ONE 9(12), 1-25.

Jothi, S., Ramakrishna Prasadand, A. Subba Reddy, M. V. 2012. Peristaltic flow of a Prandtl fluid in a symmetric channel under the effect of a magnetic field, *Advances in Applied Science Research*, 3 (4), 2108-2119.

Kh. S. Mekheimer and Elmaboud, Y. A. 2008. The influence of heat transfer and magnetic field on peristaltic transport of a Newtonian fluid in a vertical annulus: application of an endoscope, Phys. Lett. A 372(10), 1657-1665.

Kh. S. Mekheimer, S. Z. A. Husseny, Y. Abd Elmaboud, 2010. Effects of heat transfer and space porosity on peristaltic flow in a vertical asymmetric channel, *Numerical Methods for Partial Differential Equations*, 36 (4), 747-770,.

Krishna Kumari, S. V. H. N. P., Ramana Murthy, M. V., Ravi Kumar, Y. V. K. Sreenadh, S. 2011. Peristaltic pumping of a Jeffrey fluid under the effect of magnetic field in an inclined channel, *Applied Mathematical Sciences*, 5 (9), 447-458.

Kwang-Hua Chu, A. 2003. Stability of slip flows in a peristaltic transport, Europhy. Lett. 64 435.

Nadeem, S. and Akbar, N. S. 2011. Influence of heat and mass transfer on peristaltic flow of a Johnson–Segalman fluid in a vertical asymmetric channel with induced MHD, *Journal of Taiwan institute of Chemical Engineers*, 42, 58–66.

Nadeem, S., Akbar, N. S. 2010. Influence of heat transfer on peristaltic transport of a Johnson-Segalman fluid in an inclined asymmetric channel, Commun. *Non-linear Sci. Numer. Simul*., 15, 2860-2877.

Ramana Kumari, A.V. and Radhakrishnamacharya, G. 2011. Effect of slip on peristaltic transport in an inclined channel with wall effects*, Int. J. of Appl. Math and Mech*., 7 (1), 1-14.

Rami Reddy, G., Satya Narayana, P. V. and Venkataramanar, S. 2010. *Peristaltic Transport of a Conducting Fluid in an Inclined Asymmetric Channel, Applied Mathematical Sciences*, 4(35), 1729 – 1741.

Sreenadh, S., Rajender, S., Krishna Kumari, S. V. H. N. P., Ravi Kumar, Y. V. K. 2011. Flow of Herschel-Bulkley fluid in an inclined flexible channel lined with porous material under peristalsis*, Int. J. Innovative technology and Creative Engineering*, 1 (7), 24-31.

Suryanarayana, M. and Sankar Shekar Raju, G. 2010. Non-linear peristaltic pumping of Johnson-Segalman fluid in an asymmetric channel under effect of a magnetic field, Europian *Journal of Scientific Research*, 46 (1), 147-164.

****